Original Article

Folia Primatol 2014;85:77–87
DOI: 10.1159/000357526

Received: August 26, 2013
Accepted after revision: November 24, 2013
Published online: January 30, 2014

Development and Three-Dimensional Morphology of the Zygomaticotemporal Suture in Primate Skulls

Neil Curtis Ulrich Witzel Michael J. Fagan

University of Hull, Hull, UK

Key Words

Zygomaticotemporal suture · Zygomatic arch · Skull · *Macaca* · Microcomputed tomography · Suture morphology

Abstract

Cranial sutures are an essential part of the growing skull, allowing bones to increase in size during growth, with their morphology widely believed to be dictated by the forces and displacements that they experience. The zygomaticotemporal suture in primates is located in the relatively weak zygomatic arch, and externally it appears a very simple connection. However, large forces are almost certainly transmitted across this suture, suggesting that it requires some level of stability while also allowing controlled movements under high loading. Here we examine the 2- and 3-dimensional (3D) morphology of the zygomaticotemporal suture in an ontogenetic series of *Macaca fascicularis* skulls. High resolution microcomputed tomography data sets were examined, and virtual and physical 3D replicas were created to assess both structure and general stability. The zygomaticotemporal suture is much more complex than its external appearance suggests, with interlocking facets between the adjacent zygomatic and temporal bones. It appears as if some movement is permitted across the suture in younger animals, but as they approach adulthood the complexity of the suture's interlocking bone facets reaches a level where these movements become minimal.

Introduction

Skulls are constructed from many bones that are connected by fibrocellular joints at sutures [Pritchard et al., 1956; Sun et al., 2004; Jones et al., 2011] that provide free (bone) edges and enable the bones to grow in size [Koskinen et al., 1975; Sun et al., 2004]. The morphology of these free edges can vary considerably depending on

KARGER
E-Mail karger@karger.com
www.karger.com/fpr

0015–5713/14/0852–0077$39.50/0

Neil Curtis
Medical and Biological Engineering Research Group
School of Engineering, University of Hull
Hull HU6 7RX (UK)
E-Mail n.curtis@hull.ac.uk

the location within the skull, and it is thought that the morphology is strongly linked to the movements and forces experienced across the suture [Herring, 1972; Herring and Mucci, 1991; Byron et al., 2004; Sun et al., 2004]. In the skull of primates, the zygomaticotemporal suture is of particular interest because it is located within a thin rod-like part of the skull, which otherwise is generally constructed from large bony plates. Also, this suture appears in a bone that directly experiences high forces, with powerful masticatory muscles attaching along its length and opposing, stabilising fascial forces [Eisenberg and Brodie, 1965; Preuschoft and Witzel, 2004; Rodriguez-Vegas and Casado Pérez, 2004; Curtis et al., 2011]. Studies have shown both compressive and tensile strains across the zygomaticotemporal suture during feeding [Rafferty and Herring, 1999], with computer simulations suggesting that there may be relatively large ventral and lateral bending deformations due to the actions of the masseter muscle [Kupczik et al., 2007; Ross et al., 2011] – although these may be exaggerated due to the omission of stabilising soft tissue structures in the models. In addition to direct muscle forces, twisting movements and forces are also likely transmitted through the zygomatic arch (and thus through the zygomaticotemporal suture) during feeding, prey capture and fighting [Preuschoft and Witzel, 2002]. For example, such movements and forces could occur when animals bite into tough food and pull away in an attempt to tear parts off. This action would result in tensile forces on one side of the skull with countercompressive forces on the other, some of which would also be directed through the zygomatic arch. These forces would result in movements in the bending plane, as highlighted in figure 1.

Externally, the zygomaticotemporal suture appears simple, and in past research investigations it has usually been represented as a straight line transecting the zygomatic and temporal bones [Kupczik et al., 2007; Wang et al., 2012]. However, due to its important location within the skull and the potentially high forces that pass through it, one might expect there to be more complexity within this suture. Here we investigate the morphology of the zygomaticotemporal suture and aim to relate this to the forces and movements that cross it. We also assess the morphology of a series of sutures in animals of varying age to understand how the suture might change during ontogeny. To do this, we carried out a microcomputed tomography (micro-CT) analysis of the zygomaticotemporal suture of 5 macaque specimens of varying age and assessed the 2- and 3-dimensional (3D) data sets generated.

Methods

Five *Macaca fascicularis* skulls of unknown age and sex (MAC-22, -19, -94, -15, -16; Hull-York Medical School, UK) were selected, and approximate skull lengths were measured between the most anterior and most posterior points of the skull, as shown in figure 1. These animals had been used previously in dental caries experiments unrelated to the present study [Smith and Beighton, 1986, 1987]. They had skull lengths of 70 mm (MAC-22), 77 mm (MAC-19), 100 mm (MAC-94), 120 mm (MAC-15) and 135 mm (MAC-16) and were chosen to represent the development of the skull from very early stages to adulthood. The ages of the specimens were estimated based on tooth eruption [Smith et al., 1994] as viewed from plain X-ray images and micro-CT scan images and are presented in table 1. These individuals had all soft tissues intact and had been curated for approximately 20 years in various storage media: at various times alcohol, formalin, water and other unknown agents. However, the morphology of the bones that make up the zygomaticotemporal suture was not likely to be affected by these storage conditions and the specimens were therefore judged to be suitable for these analyses. The left zygomatic arch was

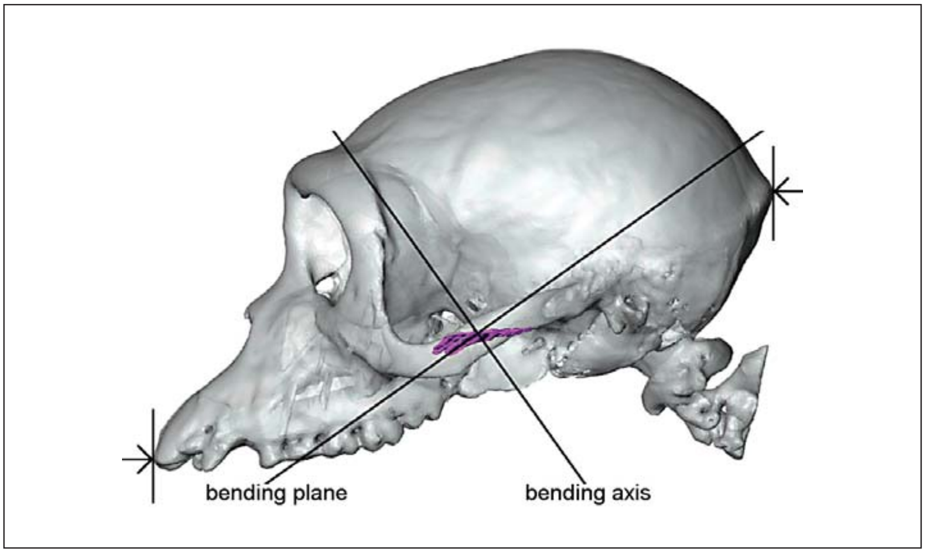

Color version available online

Fig. 1. Example skull showing the bending plane and bending axis of the zygomatic arch. Arrows represent the positions for skull length measurements. Skull aligned in the Frankfort horizontal plane.

Table 1. *Macaca* specimens used in this study

Specimen	Skull length, mm	Estimated age, years	Erupted teeth
MAC-22	70	<0.5	None
MAC-19	77	1.5–2.5	M1
MAC-94	100	3.5	I1, I2, M1, M2
MAC-15	120	>5.5	I1, I2, C, P1, P2, M1, M2, M3
MAC-16	135	>5.5	I1, I2, C, P1, P2, M1, M2, M3

I, C, P and M refer to incisor, canine, premolar and molar, respectively.

removed from each of the skulls via cuts to the zygomatic and temporal bones, ensuring the extraction of the intact zygomaticotemporal suture. The extracted arches were individually subjected to high resolution micro-CT scanning (X-Tek HMX-160 X-ray scanner; University of Hull, UK). It was necessary to remove the arches from the skulls to allow closer positioning of the sample relative to the X-ray source within the micro-CT scanner to acquire the highest possible resolution images necessary to see the complex features within the suture.

The micro-CT analysis resulted in a series of scan images (of which there were typically 1,000 individual images with a resolution of 10–20 μm). These images were imported into AVIZO image segmentation software (AVIZO v.5, VSG, USA) to allow the identification and extraction of the zygomatic and temporal bones from the greyscale images (fig. 2a). This process involved first selecting the gap between the zygomatic and temporal bones (fig. 2b) to ensure there was a distinct and complete boundary between the two bones. This required the use of a combination of the 'magic wand' and 'brush' features in the AVIZO segmentation editor. Where possible, the magic wand feature was applied to all slices in the image stack to select the gap, but this was not always possible. When the gap between the two bones was very small or the clarity of the greyscales within the image was not sufficient, the brush feature and manual segmentation were used. Next, all bone within the scan images was selected using the automatic 'thresholding' feature in AVIZO (fig. 2c), before deleting the highlighted gap area that had been identified previously (fig. 2d). This process ensured that the pixels related to the zygomatic bone within the scan images were completely separate from the pixels related to the temporal bone within the scan images, not just in the individual scan images, but also in the 3D projection when all images were interconnected. The final stage in the bone extraction procedure was to isolate the zygomatic bone from the temporal bone and register them as two separate structures (fig. 2e). It was not possible to do this segmentation process on the smallest skull arch (MAC-22) since there was little ossification and the distinction between soft tissues and bony structures was blurred (see fig. 3). From the segmented scans of each of the specimens, 3D surface models were then generated within AVIZO (for an example, see fig. 2f).

To understand better how the zygomatic and temporal bone surfaces fit together and to test general stability, plastic 3D rapid prototype (RP) models were built from the AVIZO surface

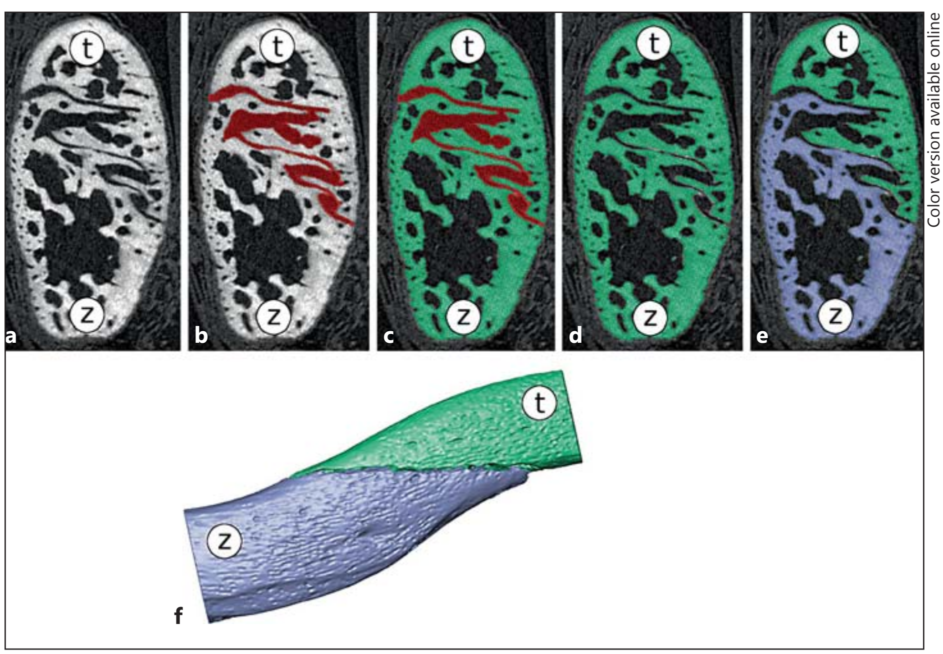

2

Fig. 2. Image segmentation procedure. Example here from MAC-94. **a** Normal unsegmented micro-CT slice image. **b** Selecting the suture gap. **c** Highlighting all the bone in the image. **d** Removing the suture gap from the selection. **e** Defining the individual bones in the image. **f** 3D reconstruction of the zygomatic (z) and temporal (t) bones.

Fig. 3. Sample micro-CT slice images from 3 representative positions across the zygomaticotemporal suture for all skulls. Not to scale. z = Zygomatic bone; t = temporal bone. Skulls aligned in the Frankfort horizontal plane. The zygomatic and temporal bones could not be identified clearly in MAC-22.

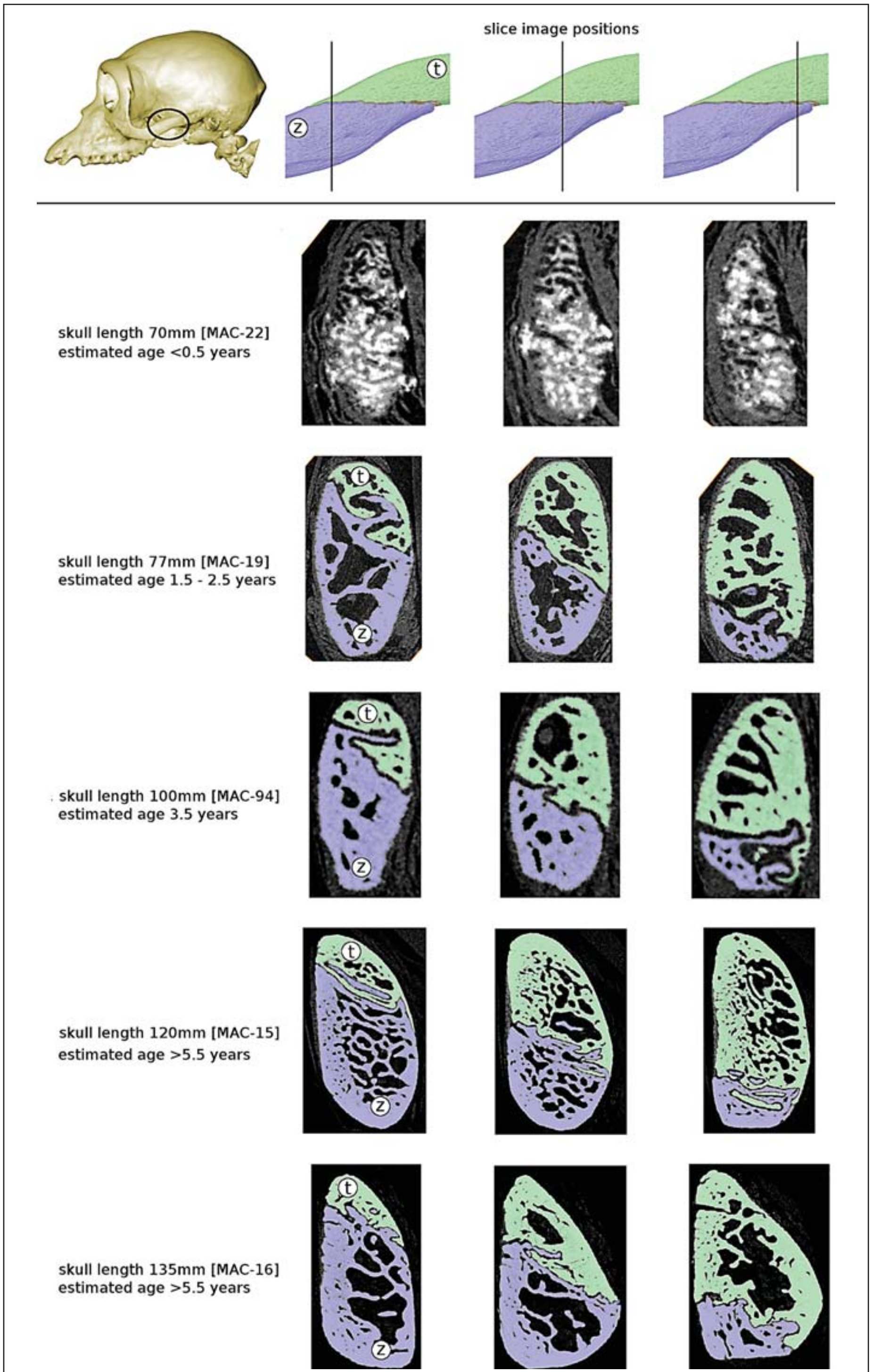

Color version available online

3

(For legend see page 80.)

models (RP machine – Eden 350, Stratsys Ltd., Rehovot, Israel; material – Objet FullCure 830 VeroWhite). To allow easier visual examination, manipulation and analysis of the plastic models, they were scaled by a factor of 5. During the rapid prototyping process, temporary scaffolds are generated automatically in the models by the RP software to ensure there is no unsupported material during the build. The scaffold material (FullCure 705 Support Resin) is water-soluble and washed away after construction. However, since the gaps between the zygomatic and temporal bones are so small and inaccessible, the removal of any scaffold structures would be very difficult if the zygomatic arch was built in one piece, even in the enlarged models. Therefore the zygomatic and temporal bones were generated as two separate models and re-articulated after construction. After manufacture and cleaning, it was found that the RP zygomatic and temporal bones of MAC-19 and MAC-94 could be re-articulated easily, but those of MAC-15 could not. Since the morphology of MAC-16 was visually more complex than that of MAC-15, a physical model of MAC-16 was not built to avoid waste of time and expense. Also, as mentioned previously, no model of MAC-22 was built since the zygomatic and temporal bones could not be identified as separate structures in the micro-CT data set and thus no 3D models could be generated.

Results

When viewed medially, the border of all sutures (i.e. the visible external line where the zygomatic and temporal bones meet) was relatively straight and lay in line with the horizontal axis when the skull was aligned in the Frankfort horizontal plane (fig. 4). In lateral view, the visible suture boundary was less straight and horizontal in appearance when compared to the medial view, and it tended to lie lower on the arch and curved upwards as it approached the arch apex. Internally, the morphology of the sutures was considerably more complex than the external appearance suggested (fig. 3–6). The suture line (or gap between the zygomatic and temporal bones) meandered and snaked its way through the suture, creating interlinking forms between the two bones (fig. 3).

3D reconstructions of the arches reveal the true morphology of the internal bone surfaces. There are clear facets that protrude from the bone, which interlink the zygomatic and temporal bones (fig. 4–6). As the animals age, the complexity of the zygomaticotemporal suture increases, with more bone facets and less uniform facets being laid down (fig. 5, 6). The depth of the facets also decreases with age, suggesting less axial movements within the suture, and combined with the greater facet complexity implies a more stable arch.

The earliest macaque arch in this study (MAC-22, estimated age <0.5 years) had low levels of ossification, and no 3D reconstructions could be generated from the micro-CT scans (fig. 3). MAC-19 was the next arch in the series and came from a macaque with a skull length of 77 mm with an estimated age of 1.5–2.5 years. The micro-CT slice data showed a relatively simple zygomaticotemporal suture with a clear separation between the zygomatic and temporal bones. The 3D reconstruction revealed 4 main interlinking facets (fig. 4–6). From a medial view, the temporal bone interlinked with the zygomatic bone by over 4 mm from the suture boundary, but viewed laterally, the lower suture boundary meant the zygomatic bone overlapped the temporal bone (fig. 4). The same trend was noted for all arches; however, the number of bone facets increased as the animal aged. There were approximately 7–8 consistently aligned facets in MAC-94 (skull length 100 mm; estimated age 3.5 years) with interlinking of about 5 mm, 13–15 clear facets in MAC-15 (not as consistently aligned as in MAC-94; skull length 120 mm; esti-

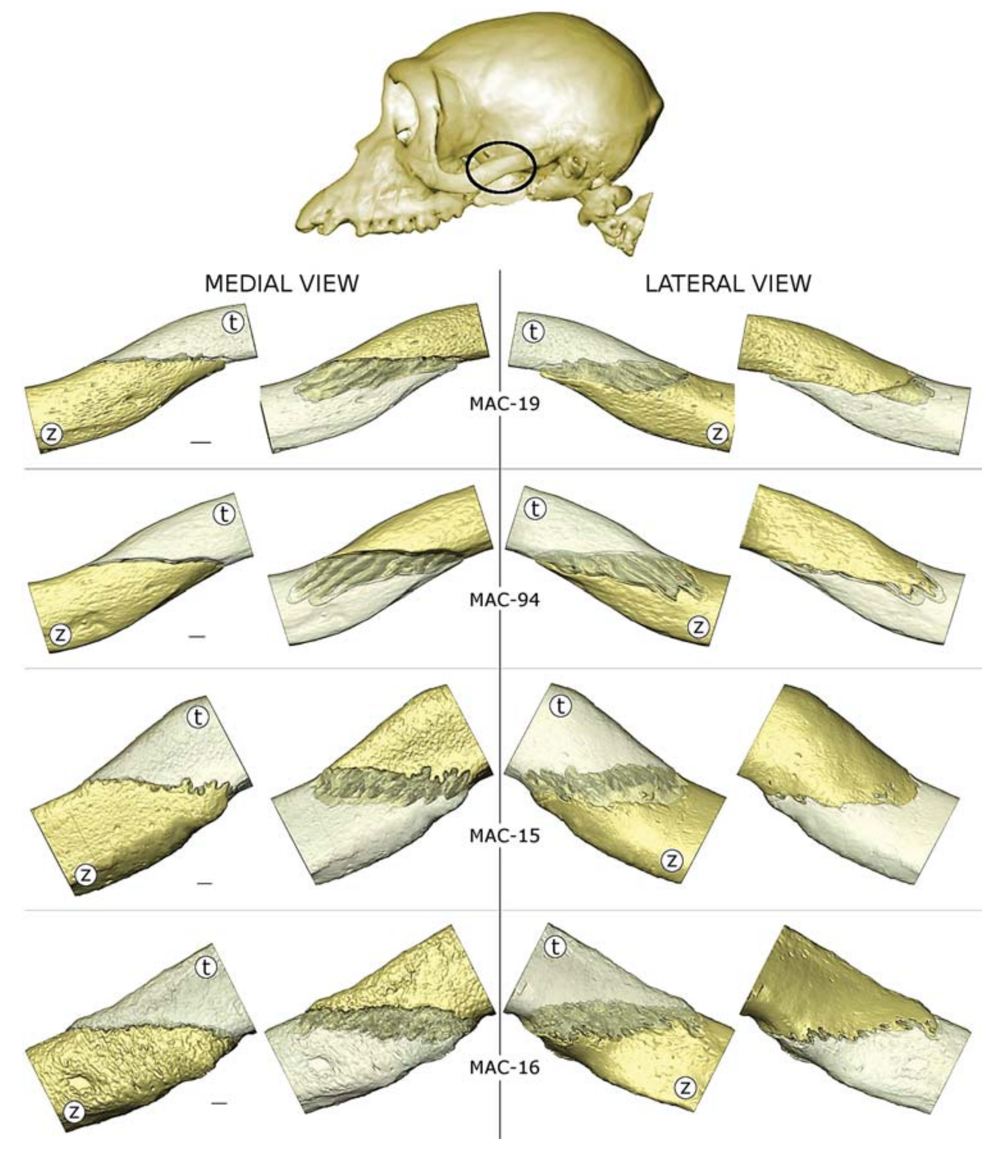

Fig. 4. Medial and lateral views showing either transparent zygomatic or temporal bones to highlight their overlap across the suture. Scale bar = 1 mm. z = Zygomatic bone; t = temporal bone. Skull and bones aligned in the Frankfort horizontal plane. More visual representations of the sutures are presented in animations in the supplementary material, see www.karger.com/doi/10.1159/000357526. A 3D model of MAC-22 could not be generated.

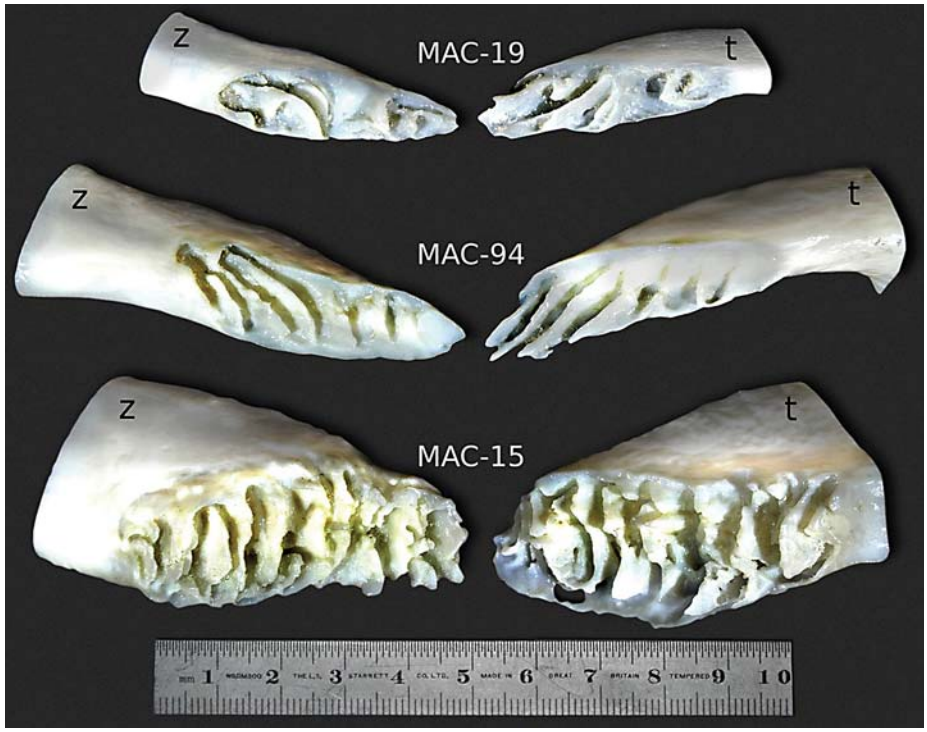

Color version available online

Fig. 5. Physical RP models of MAC-19, MAC-94 and MAC-15. These models were scaled to 5 times original size. The zygomatic bones have been rotated/flipped to show the suture morphology. z = Zygomatic bone; t = temporal bone. No RPs of MAC-22 or MAC-16 were created.

mated age >5.5 years) with interlinking of typically 3 mm, and >10 more sporadically aligned facets in MAC-16 (skull length 135 mm; estimated age >5.5 years) with typically 2 mm of interlinking. Furthermore, in MAC-16 there were more obvious smaller facets around the perimeter of the zygomatic and temporal bones suggesting more interlinking at the suture boundary (fig. 6). Using the surface area measurement tool in AVIZO, and assuming that the thickness of each suture was negligibly small, we estimated that the mean surface areas (i.e. the total surface area of the suture volume divided by 2) of the zygomatic and temporal bone facets of the suture were 37.5, 62.0, 182.5 and 123.0 mm^2 for MAC-19, -94, -15 and -16, respectively, highlighting the increased complexity of the bone surfaces as the animal ages. This increased surface area would increase the area for ligamentous attachment within the suture, which would increase the stiffness of the joint (for all online suppl. videos (1–4), see www.karger.com/doi/10.1159/000357526 for animations of the sutures, showing the 3D volume of the suture gap and the morphology of the suture as several positions along its length).

The following description is based on manual manipulation of the RP models of MAC-19 and MAC-94 to assess the stability of the joints. There was an obvious compressive constraint when the zygomatic and temporal bones were pushed together,

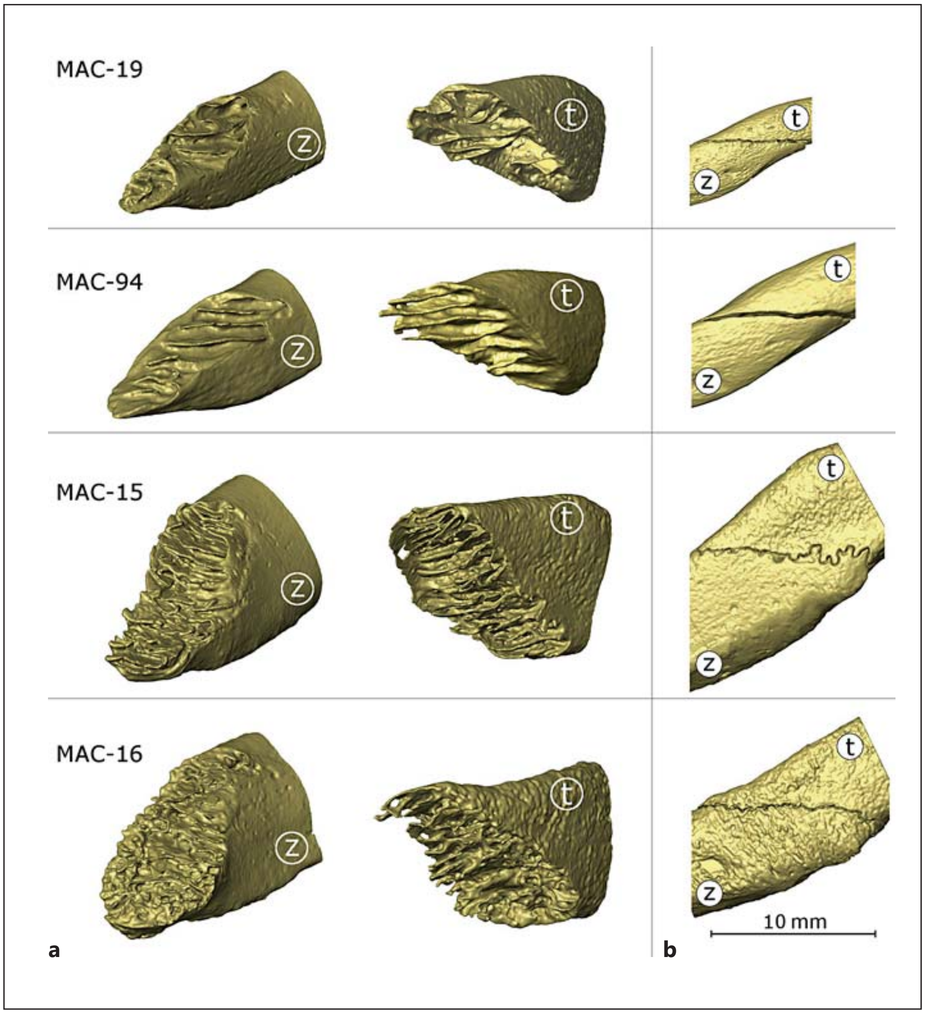

Color version available online

Fig. 6. 3D surface models of all zygomatic arches. **a** Exploded views positioned and scaled to best show the 3D geometries of the bone surfaces (not to scale). **b** Sections of each arch showing the zygomaticotemporal suture line (medial view, all arches scaled proportionally to allow comparison of sizes). z = Zygomatic bone; t = temporal bone. A 3D model of MAC-22 could not be generated.

and the bones locked in a stable condition. Under tension, a small degree of movement guided by the bone facets of a number of lamellae was possible until a definite stop on this movement was detected. This stop was due to slight variations in the alignment of the facets and the presence of smaller cross-facets that were engaged when the zygomatic and temporal bones moved apart. In the bending plane (fig. 1), the arch was stable under medially directed forces due to the closed geometry of the bone facets, but the geometric constraints to lateral forces in this bending plane appear to be less substantial.

Discussion

The zygomaticotemporal suture is considered to be a simple joint and is often represented as a straight cut through the zygomatic arch [Kupczik et al., 2007; Wang et al., 2012]. However, this investigation shows that this is not the case. The zygomaticotemporal suture in *Macaca fascicularis* is complex, with organised bone facets that constrain movements between the zygomatic and temporal bones. Excluding the earliest individual in this study (MAC-22), which shows little ossification, it appears that the zygomatic and temporal bones are able to slide relative to each other along the direction of the bone planes. However, as the animal ages, the complexity of the bony surfaces increases to a point where motion seems less likely (e.g. as in MAC-15 and MAC-16). There is also the possibility of additional rotational movement in the plane of the bony interdigitations, due to the lack of apparent constraining structures on the medial aspect of the arch.

Since no soft tissue structures are included in the RP models, all movements noted during manual manipulation must be viewed as extreme. In reality there are collagen fibres that would restrain movements [Pritchard et al., 1956; Jaslow, 1990; Cohen, 2000], and during tensile translations these fibres would store energy and help return the suture to its original position. That being said, the movements noted during the manual manipulation of the physical models were defined purely by the geometries of the zygomatic and temporal bone surfaces, and thus must be representative of the degrees of freedom permitted across the suture. We have shown here that the zygomaticotemporal suture is complex, with this complexity increasing with age. As the animal matures, the size and stiffness of the rest of the cranium can be expected to increase so that the tensile and bending movements at the zygomaticotemporal suture may also reduce. As a result, the zygomatic and temporal bone surfaces may approach a state where they become interlocked, as observed with the 2 oldest specimens (>5.5 years MAC-15 and MAC-16) in this study.

Small amounts of tensile and rotational freedom at the zygomaticotemporal suture could be very important in the protection of the zygomatic arch when bending stresses are focused on this region; for example, any lateral pulling movements at the jaw when pulling against food will impose a bending moment within the skull. Due to its extreme lateral positioning on the skull, the zygomatic arch on one side will undergo compressive stresses, while the opposing arch will undergo tensile stresses [Witzel et al., 2004]. The degrees of freedom permitted at the zygomaticotemporal suture are well suited to resist these stresses, with the apparent small relative movements between the zygomatic and temporal bones offering the potential to reduce the tensile stresses in the zygomatic arch. However, while some freedom may be desirable, the arch must also be stable when forces are applied across it. For example, forces from the masseter muscle combined with the temporal fascia [Preuschoft and Witzel, 2004; Witzel et al., 2004; Curtis et al., 2011] apply a medially directed resultant force to the arch. The arch must not buckle or dislocate under this force. We saw from manual manipulation of the RP models of MAC-19 and MAC-94 that the arch was stable against such forces, even when some additional degree of tensile movement was applied.

We recognise that this study is limited in that it considers only a small number of samples and only 1 species. However, the complexity of the bony surfaces certainly appears to increase with age in a consistent way, and we expect therefore that these results will be confirmed in a larger study. It would be interesting to examine the variability of the suture's complexity in individuals of the same age, and to compare the structure of the zygomaticotemporal suture in different primates and other animals, with a range of feeding habits.

Acknowledgements

The first author was funded by the Leverhulme Trust. We are very grateful to Paul O'Higgins and Hull-York Medical School for access to the material used in this study, and to Laura Fitton (Hull-York Medical School) for her help in determining the specimens' ages.

References

Byron CD, Borke J, Yu J, Pashley D, Wingard CJ, Hamrick M (2004). Effects of increased muscle mass on mouse sagittal suture morphology and mechanics. *The Anatomical Record* 279: 676–684.
Cohen MM (2000). Sutural biology, chapter 2. In *Craniosynostosis* (Cohen MM, Mclean RE, eds.). Oxford, University Press.
Curtis N, Witzel U, Fitton L, O'Higgins P, Fagan MJ (2011). The mechanical significance of the temporal fasciae in *Macaca fascicularis*: an investigation using finite element analysis. *The Anatomical Record* 294: 1178–1190.
Eisenberg NA, Brodie AG (1965). Antagonism of temporal fascia to masseteric contraction. *The Anatomical Record* 152: 185–192.
Herring SW (1972). Sutures – a tool in functional cranial analysis. *Acta Anatomica* 83: 222–247.
Herring SW, Mucci RJ (1991). In vivo strain in cranial sutures: the zygomatic arch. *Journal of Morphology* 207: 225–239.
Jaslow CR (1990). Mechanical properties of cranial sutures. *Journal of Biomechanics* 23: 313–321.
Jones MEH, Curtis N, Fagan MJ, O'Higgins P, Evans SE (2011). Hard tissue anatomy of the cranial joints in *Sphenodon* (Rhynchocephalia): sutures, kinesis, and skull mechanics. *Palaeontologia Electronica* 14: 17A.
Koskinen L, Isotupa K, Kosko K (1975). A note on craniofacial suture growth. *American Journal of Physical Anthropology* 45: 511–516.
Kupczik K, Dobson CA, Fagan MJ, Crompton RH, Oxnard CE, O'Higgins P (2007). Assessing mechanical function of the zygomatic region in macaques: validation and sensitivity testing of finite element models. *Journal of Anatomy* 210: 41–53.
Preuschoft H, Witzel U (2002). Biomechanical investigations on the skulls of reptiles and mammals. *Senckenbergiana Lethaea* 82: 207–222.
Preuschoft H, Witzel U (2004). A biomechanical approach to craniofacial shape in primates, using FESA. *Annals of Anatomy* 186: 397–404.
Pritchard JJ, Scott JH, Girgis FG (1956). The structure and development of cranial and facial sutures. *Journal of Anatomy* 90: 73–86.
Rafferty KL, Herring SW (1999). Craniofacial sutures: morphology, growth, and in vivo masticatory strains. *Journal of Morphology* 242: 167–179.
Rodriguez-Vegas JM, Casado Pérez C (2004). Inexpensive custom-made external splint for isolated closed zygomatic arch fractures. *Plastic and Reconstructive Surgery* 113: 1517–1518.
Ross CF, Berthaume MA, Dechow PC, Iriarte-Diaz J, Porro LB, Richmond BG, Spencer MA, Strait DS (2011). In vivo bone strain and finite-element modelling of the craniofacial haft in catarrhine primates. *Journal of Anatomy* 218: 112–141.
Smith BH, Crummett TL, Kari LB (1994). Ages of eruption of primate teeth: a compendium for aging individuals and comparing life histories. *Americal Journal of Physical Anthropology* 37: 177–231.
Smith K, Beighton D (1986). The effects of the availability of diet on the levels of exoglycosidases in the supragingival plaque of macaque monkeys. *Journal of Dental Research* 65: 1349–1352.
Smith K, Beighton D (1987). Proteolytic activities in the supragingival plaque of monkeys *(Macaca fascicularis)*. *Archives of Oral Biology* 32: 473–476.
Sun Z, Lee E, Herring SW (2004). Cranial sutures and bones: growth and fusion in relation to masticatory strain. *The Anatomical Record* 276A: 150–161.
Wang Q, Wood SA, Grosse IR, et al. (2012). The role of the sutures in biomechanical dynamic simulation of a macaque cranial finite element model: implications for the evolution of craniofacial form. *The Anatomical Record* 295: 278–288.
Witzel U, Preuschoft H, Sick H (2004). The role of the zygomatic arch in the statics of the skull and its adaptive shape. *Folia Primatologica* 75: 202–218.